32ND INTERNATIONAL COSMIC RAY CONFERENCE, BEIJING 2011

Measurement of UHECR Mass Composition by TA FD Stereo

YUICHIRO TAMEDA[1], MASAKI FUKUSHIMA[1], DAISUKE IKEDA[1], FUMIO KAKIMOTO[2], YOSHIKI TSUNESADA[2], HISAO TOKUNO[2], KENTARO HAYASHI[2], SHOICHI OGIO[3], TOSHIHIRO FUJII[3] AND THE TA COLLABORATION

[1]*Institute for Cosmic Ray Research, The University of Tokyo, Kashiwa, Chiba, Japan,*
[2]*Graduate School of Science and Engineering, Tokyo Institute of Technology, Meguro, Tokyo, Japan,*
[3]*Graduate School of Science, Osaka City University, Sumiyoshi, Osaka, Japan*
tame@icrr.u-tokyo.ac.jp
DOI: 10.7529/ICRC2011/V02/1268

Abstract: The Telescope Array is a hybrid detector consisting of Fluorescence Detectors (FDs) and Surface Detectors (SDs) to observe Ultra High Energy Cosmic Rays (UHECRs). FDs can measure longitudinal developments of cosmic-ray air showers directly. Xmax is the shower parameter that depends most on cosmic ray primary particle type. In this presentation, the most recent Xmax analysis of UHECR mass composition measured by TA FD stereo will be reported.

Keywords:

1 Introduction

In order to understand ultra-high energy cosmic rays (UHECRs), it is important to understand the origin of them. UHECRs with energies around 10^{20}eV do not deflect much in the galactic magnetic field [1]; therefore, they can be traced back to their sources. This means that UHECRs have a potential to be used for charged particle astronomy.

So far, three experiments have reported on the mass composition of UHECRs: AGASA indicated no composition change above $10^{17.5}$eV based on the relation between the number of shower muons and electrons [2], and HiRes reported results consistent with a proton dominated composition between 1.6 and 64EeV based on the average $X_{\max}$ technique [3]. On the other hand, the Pierre Auger Observatory (PAO) reports that while the composition is proton dominated between $10^{18.0}$eV and $10^{18.5}$eV, above that it seems to be getting heavier [4]. They base this on how the average $X_{\max}$ and the RMS of $X_{\max}$ changes with energy. However, the PAO claims that UHECR arrival directions correlate with some AGNs [5] suggests that the composition should be light nuclei.

The mass composition of UHECR is indispensable for the interpretation of not only UHECR sources, but also the structure of the energy spectrum and for anisotropy. For example, if UHECR mass composition is dominated by protons, then the ankle structure in the spectrum might be understood as a result of e^-/e^+ pair production due to the proton's interaction with the cosmic microwave background [6]. Furthermore, how well one can trace UHECR arrival directions back to the source after passing through galactic or extra-galactic magnetic fields depends strongly on the mass composition, which is a crucial point for anisotropy studies.

The Telescope Array (TA) is a hybrid detector consisting of a Surface Detector (SD) array and Fluorescence Detectors (FD) to observe UHECRs. It is located in the western desert of Utah. The SD array consists of 507 three square meter plastic scintillation counters arranged on a 1.2km grid for a detection area of $\sim 700\mathrm{km}^2$, 7 times larger than AGASA. There are three FD stations overlooking the SD array. Two of the FD stations contain 12 newly developed FD telescopes each, the other contains 14 telescopes transferred from HiRes-1. TA has been taking data with all detectors since May 2008.

2 Mass Composition Analysis

2.1 $X_{\max}$ Technique

The longitudinal development of a cosmic ray air shower depends strongly on its primary energy and particle type. The depth in the atmosphere at which the number of particles in the shower reaches a maximum, $X_{\max}$, is a good indicator of primary particle type. Since an FD observes longitudinal development of air showers, this technique has the advantage over SDs of measuring the energy calorimetrically and being able to determine primary particle type.

The mass composition cannot be determined on a shower by shower basis due to fluctuations in development of individual showers, but it can be determined on a statistical

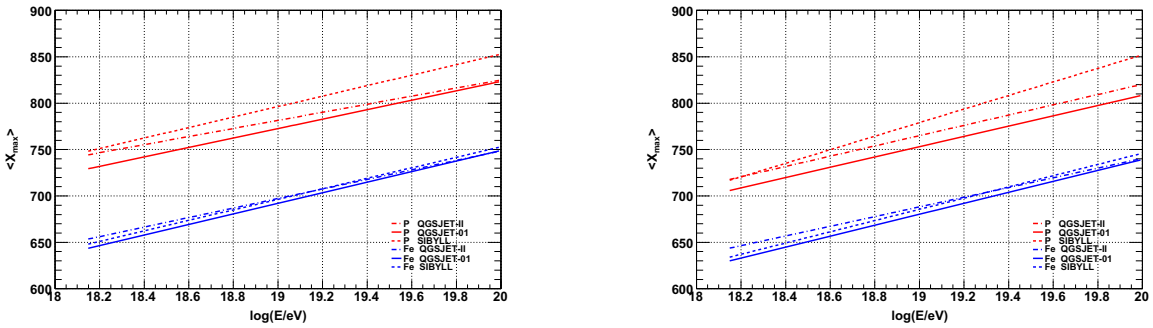

Figure 1: Left: Averaged $X_{\max}$ estimated by CORSIKA. Right: Expected averaged $X_{\max}$ observed by TA FD. Primary particles are protons (red) or iron nuclei (blue). Hadronic interaction models are QGSJET-01, QGSJET-II and SIBYLL.

basis by comparing the $X_{\max}$ distribution of the data from many showers and the distribution expected from a monte carlo (MC) simulation. However, it should be noted that the uncertainty of the MC depends strongly on hadron interaction models that have been extrapolated from measured cross sections at much lower energies.

As energy increases, the $X_{\max}$ of air showers increase. And at a given energy, the $X_{\max}$ of a light primary particle will be deeper than that of a heavy primary particle. Since the FDs only can see showers in certain geometric regions, the $X_{\max}$ may be either above the field of view (FOV) or below it, or it may be inside the field of view but the FD cannot reconstruct the shower (for instance, the shower may be coming nearlydirectly toward the FD). In these cases one cannot assign an $X_{\max}$ to the shower. This means that the distribution of observed $X_{\max}$ will be different from the expected distribution unless the FD configuration is taken into account in the simulation. In this analysis, the $X_{\max}$ distribution affected by the detector configuration and shower reconstruction biases will be estimated and compared with data to determine UHECR mass composition.

2.2 Shower Simulation

The distribution of $X_{\max}$ for each energy bin is estimated with a MC shower simulation using CORSIKA (ver 6.972) [7]. QGSJET-01, QGSJET-II and SIBYLL are used for the hadronic interaction models. To reduce computation time, thinning is applied with a thinning factor $\varepsilon = 10^{-4}$ and weighting limitations of $w(e.g.) = \varepsilon \times E_0(\mathrm{GeV})$ for electrons and gammas, and $w(m.h.) = w(e.g.)/100$ for muons and hadrons, where E_0 is the primary energy. The thinning factor and weighting limitations were chosen to produce smooth shower development. The energy below which the simulation no longer follows particles is $100\mathrm{keV}$ for the hadronic component and $100\mathrm{MeV}$ for the electromagnetic component.

The shower library used for the expected distributions is generated using a primary energy between $10^{18}\mathrm{eV}$ and $10^{20}\mathrm{eV}$. The zenith angle is chosen between 0 and 65 deg randomly. The shower development is only followed to the median elevation of the TA site of 1400 m asl. Primary particles are assumed to be either protons or iron nuclei. The left side of Fig. 1 shows the average $X_{\max}$ for each energy bin based on the shower MC simulation. This $X_{\max}$ distribution still cannot be compared directly with the observed data because the simulation at this point still does not reflect the detector response or reconstruction procedure used for the data.

2.3 Detector Simulation

The expected distributions of the UHECRs primary energy and $X_{\max}$, and the systematics of the TA FD shower reconstruction procedure are estimated by the detector simulation using the shower library generated by CORSIKA in the previous section. The detector simulation proceeds as follows: First the amount of fluorescence light and cherenkov emission along the shower axis is estimated from the energy deposited and numbers of shower particles at various depths along the shower. Although the ratio of Cherenkov light to total light that hits the FDs directly is very small due to the directionality of the cherenkov photons, the contribution of scattered (Rayleigh and aerosol) cherenkov light becomes larger around the depth of shower maximum. So scattered cherenkov light needs to be taken into account in order not to overestimate $X_{\max}$ and Nmax. Next, for each shower geometry, the shower core is placed randomly within a circle of radius 20 km of the center of the field of view of the FD stereo aperture. Then the expected FADC counts caused by photons from a shower axis are estimated taking into account atmospheric attenuation, actual detector configuration, mirror reflectivity, gains of PMTs, *etc.* Finally, the energy and $X_{\max}$ distribution is estimated from the simulated showers that pass the same reconstruction cuts as used in the observed data. The right side of Fig. 1 shows the average $X_{\max}$ that is expected to be observed by TA FD for either proton or iron primaries. This average $X_{\max}$ includes biases due to both the detector's acceptance and shower reconstruction.

The reconstruction accuracy is estimated by comparing the actual and reconstructed values for MC showers. The determination of arrival directions and positions of the shower core at $E_0 > 10^{19}$eV are ± 1.88 deg and ± 250 m respectively. The energy determination is $1.6 \pm 7.6\%$ for proton. The $X_{\rm max}$ accuracy is $-6.2 \pm 22 {\rm g/cm}^2$ for proton. The total energy deposited which is calculated by integration of the Gaisser-Hillas function along the shower axis is 93 % for protons and 89 % for iron.

3 Results

The mass composition of UHECR can be determined by data/MC comparison of $X_{\rm max}$. MC must reflect the actual detector configuration, atmospheric profile, triggering requirements, etc. The atmospheric profile used was the monthly average of the radiosonde launched at Elko, Nevada, which is the closest launch site to TA. The distribution of aerosols was measured at the TA site by LIDAR [8]. Data was observed in stereo from Nov 2007 to Sep 2010.

For the determination of mass composition, both the average $X_{\rm max}$ and the distribution of $X_{\rm max}$ can be used. In Fig. 2 the average $X_{\rm max}$ data is consistent with the prediction expected for protons primaries based on the QGSJET-II hadron interaction model. Moreover, there is no evidence in Fig. 2 of any bend in the variation of average $X_{\rm max}$ with energy, which suggests that mass composition does not change in this energy region.

Figure 3 shows comparisons of $X_{\rm max}$ distribution between data and MC for each energy bin. The distributions are consistent with proton primaries, although at high energies the statistics are low. In order to estimate the agreement of $X_{\rm max}$, Kolmogorov-Smirnov (KS) test is applied to these $X_{\rm max}$ distribution. The result of KS test is shown in Fig. 4. For any hadron interaction models, $X_{\rm max}$ distributions of proton primary model are compatible with data. On the other hand, p-values of iron primary model are much lower than that of proton model in the energy region between $10^{18.2}$ and $10^{19.4}$eV. In this energy region, iron primary model can be rejected with 95% confidence level (CL). However, above the energy of $10^{19.4}$eV, p-values of iron model are still high. This means that above $10^{19.4}$eV both models are consistent with data with this statistics.

TA FD stereo data is consistent with proton primary model of especially QGSJET based on averaged $X_{\rm max}$ analysis. The highest energy bin looks iron but it should not be concluded as iron due to low statistics of one event. According to the result of KS test applied to $X_{\rm max}$ distribution, data is consistent with proton model for whole energy region with 95% CL and iron primary model can be rejected at least the energy region between $10^{18.2}$ and $10^{19.4}$eV. However, data is also consistent with iron primary model above $10^{19.4}$eV due to the low statistics, though averaged $X_{\rm max}$ looks proton like. In order to conclude for above $10^{19.4}$eV, we need more statics.

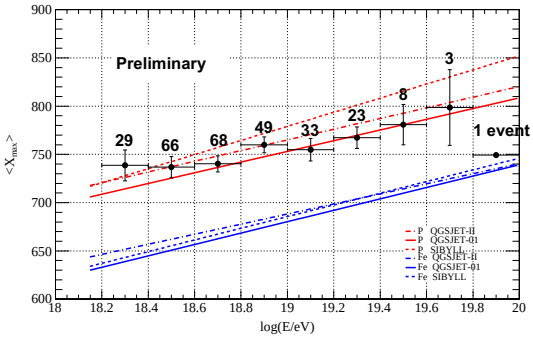

Figure 2: Averaged $X_{\rm max}$ of MC and Data. MC prediction rails include biases estimated by detector simulation. Red and blue lines are proton or iron, respectively and hadron interaction models are QGSJET-01, QGSJET-II and SIBYLL.

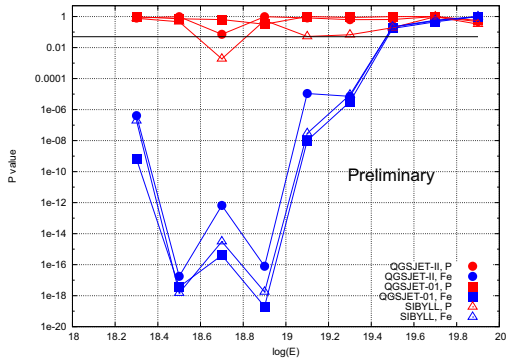

Figure 4: P-values estimated by KS test applied to $X_{\rm max}$ distribution for each primary particle type, hadronic interaction model and each energy region.

Acknowledgements

The Telescope Array experiment is supported by the Japan Society for the Promotion of Science through Grants-in-Aid for Scientific Research on Specially Promoted Research (21000002) "Extreme Phenomena in the Universe Explored by Highest Energy Cosmic Rays", basic research awards 18204020(A), 18403004(B) and 20340057(B); by the U.S. National Science Foundation awards PHY-0307098, PHY-0601915, PHY-0703893, PHY-0758342, and PHY-0848320 (Utah) and PHY-0649681 (Rutgers); by the National Research Foundation of Korea (2006-0050031, 2007-0056005, 2007-0093860, 2010-0011378, 2010-0028071, R32-10130); by the Russian Academy of Sciences, RFBR grants 10-02-01406a and 11-02-01528a (INR), IISN project No. 4.4509.10 and Belgian Science Policy under IUAP VI/11 (ULB). The foundations of Dr. Ezekiel R. and Edna Wattis Dumke, Willard L. Eccles and the George S. and Dolores Dore Eccles all helped with generous donations. The State of Utah supported the project through its Economic Development Board, and the Univer-

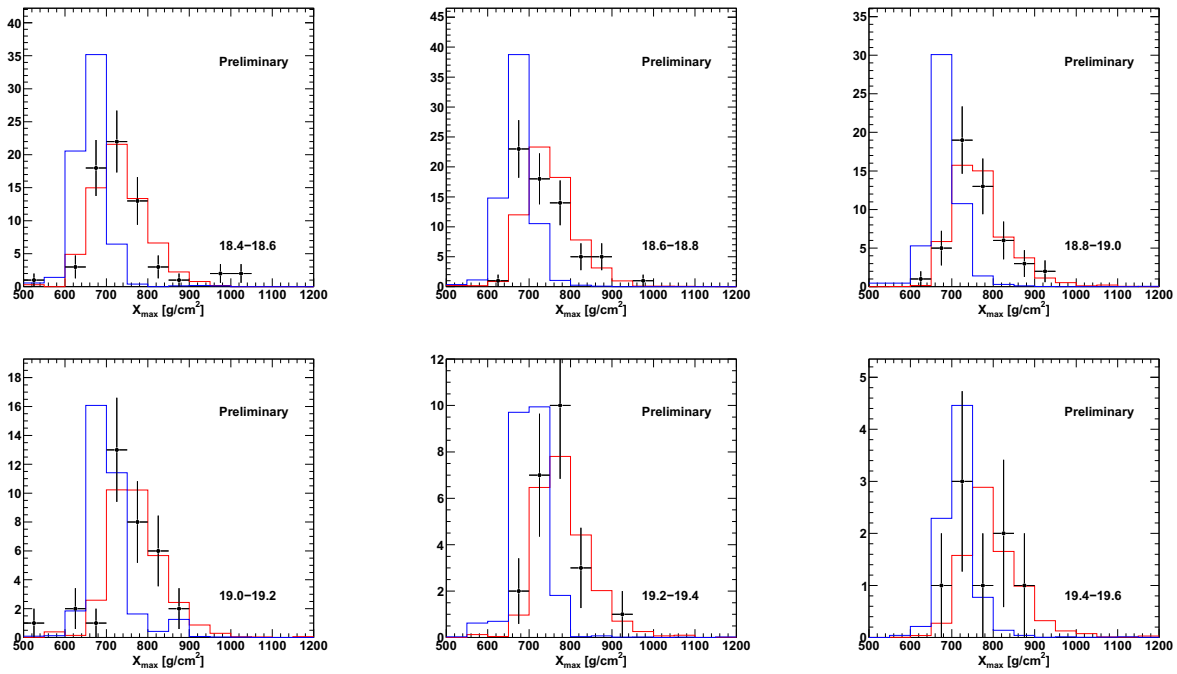

Figure 3: MC/Data comparison of $X_{\max}$ distribution for each energy region. Black points are data. Red and blue histogram are MC for proton and iron primary, respectively. These MC are based on the QGSJET-II.

sity of Utah through the Office of the Vice President for Research. The experimental site became available through the cooperation of the Utah School and Institutional Trust Lands Administration (SITLA), U.S. Bureau of Land Management and the U.S. Air Force. We also wish to thank the people and the officials of Millard County, Utah, for their steadfast and warm support. We gratefully acknowledge the contributions from the technical staffs of our home institutions and the University of Utah Center for High Performance Computing (CHPC).

References

[1] J.W. Cronin, Nucl. Phys. B Proc. Supp., 2005, **138**: 465-491
[2] Hayashida et al.,N , J. Phys. G, 1995, **21**: 1101-1119
[3] R.U. Abbasi et al., Phys. Rev. Lett., 2010, **104**: 161101
[4] J. Abraham et al., Phys. Rev. Lett., 2010, **104**: 091101
[5] The Pierre Auger Collaboration, Science, 2007, **318**: 938-943
[6] V. Berezinsky et al., Phys. Lett. B, 2005, **612**: 147 - 153
[7] D. Heck al et., Report FZKA 6019, 1998
[8] T. Tomida et al., 31th ICRC, Lodz, Poland, 2009